The Spine Journal 19 (2019) 1242–1253

Basic Science

Assessment of changes in the micro-nano environment of intervertebral disc degeneration based on Pfirrmann grade

Yan-Jun Che, MD, PhD[a,b], Jiang-Bo Guo, MD[a], Ting Liang, PhD[a], Xi Chen, PhD[a], Wen Zhang, PhD[a], Hui-Lin Yang, MD, PhD[a], Zong-Ping Luo, PhD[a,*]

[a] *Orthopaedic Institute, Department of Orthopaedics, The First Affiliated Hospital of SooChow University, 708 Renmin Rd, SuZhou, Jiangsu 215007, PR China*

[b] *Department of Orthopedics, The Affiliated Peace Hospital of Changzhi Medical College, 110 Yan'an Rd, Changzhi, Shanxi 046000, PR China*

Received 2 November 2018; revised 26 January 2019; accepted 28 January 2019

Abstract

BACKGROUND CONTEXT: Pfirrmann grading can be used to assess intervertebral disc degeneration (IVDD). There is growing evidence that IVDD is not simply a structural disorder but also involves changes to the substructural characteristics of the disc. Whether Pfirrmann grade can accurately represent these micro-nano environmental changes remains unclear.

PURPOSE: We aimed to assess the micro-nano structural characteristics of the degenerative disc to provide more specific biomechanical information than the Pfirrmann score.

STUDY DESIGN: A micro- and nano-level structural analysis of degenerative discs of rat tails.

METHODS: In this study, 12-week-old adult male Sprague-Dawley rats were divided randomly into five groups: control (no intervention to the intervertebral disc of the tail) and four intervention groups that all had caudal vertebrae immobilized using a custom-made external device to fix four caudal vertebrae (Co7–Co10) but with variable subsequent compression of Co8 and Co9 for 2, 4, 6, or 8 weeks. Magnetic resonance imaging detection of rat coccygeal vertebrae was conducted at each time node of the experiment, and the T2 signal intensity and disc space were evaluated. Animals were euthanized and the caudal vertebrae were harvested for further analysis. Histopathology, glycosaminoglycan (GAG) content, histologic score, end plate structure, and elastic modulus of the intervertebral discs were evaluated.

RESULTS: IVDD was observed at an earlier Pfirrmann grade (Pfirrmann II) under the microscope. With an increase in Pfirrmann grade to III–V, the pore structure of the bony end plate changed significantly and the number of pores decreased gradually. Furthermore, the total GAG content of the nucleus pulposus decreased from an average of 640.33 μg GAG/ng DNA in Pfirrmann grade I to 271.33 μg GAG/ng DNA in Pfirrmann grade V ($p < .0001$). At the early stage of clinical degeneration of intervertebral discs (Pfirrmann grades II and III), there were significant changes in mechanical properties of the outer annulus fibrosus compared with the inner layer ($p < .05$). Further, the fibril diameters exhibited significant changes compared with the control group ($p < .05$).

CONCLUSIONS: Our study found that the Pfirrmann grading system combined with intervertebral disc micro-nano structural changes more comprehensively reflected the extent of disc

FDA device/drug status: Not applicable.

Author disclosures: ***YJC:*** Grants: National Natural Science Foundation of China and Basic Research Program of Jiangsu Province (G, paid directly to institution). ***JBG:*** Grants: National Natural Science Foundation of China and Basic Research Program of Jiangsu Province (G, paid directly to institution). ***TL:*** Grants: National Natural Science Foundation of China and Basic Research Program of Jiangsu Province (G, paid directly to institution). ***XC:*** Grants: National Natural Science Foundation of China and Basic Research Program of Jiangsu Province (G, paid directly to institution). ***WZ:*** Grants: National Natural Science Foundation of China and Basic Research Program of Jiangsu Province (G, paid directly to institution). ***HLY:*** Grants: National Natural Science Foundation of China and Basic Research Program of Jiangsu Province (G, paid directly to institution). ***ZPL:*** Grants: National Natural Science Foundation of China and Basic Research Program of Jiangsu Province (G, paid directly to institution).

* Corresponding author. Orthopaedic Institute, Department of Orthopaedics, The First Affiliated Hospital of SooChow University, 708 Renmin Rd, SuZhou, Jiangsu 215007, PR China. Tel.: 86-512-6778-1351; fax: 86-512-6778-1165.

E-mail address: zongping_luo@yahoo.com (Z.-P. Luo).

https://doi.org/10.1016/j.spinee.2019.01.008

degeneration. These data may help improve our understanding of the pathogenesis and process of clinical disc degeneration.

Keywords: Pfirrmann grade; Micro-nano environment; Biomechanics; Intervertebral disc degeneration; Intervertebral disc substructure; Rat model

Introduction

The grading of intervertebral disc degeneration (IVDD) is commonly performed using the Pfirrmann system [1−3]. This system is based on T2-weighted magnetic resonance imaging (MRI), which essentially assesses water content based on signal intensity [4,5]. The degree of IVDD is evaluated according to the morphologic structure of the disc, and assigned one of five grades (I−V). It is suitable for preoperative evaluation of the degree of degeneration and also allows horizontal comparison between different studies. However, there are some limitations. First, it is difficult to distinguish the early degenerative changes using the integer-based Pfirrmann score [6,7]. Second, the grading system is qualitative and more or less subjective, which can be affected by observer error, especially in relation to the intervertebral disc substructure. Third, correlation between the Pfirrmann grade and the occurrence or severity of clinical symptoms is poor.

It is established that each substructure of the intervertebral disc has its own specific mechanical properties. Degeneration affects these properties and impacts on the mechanical function of the entire intervertebral disc. That is, the mechanical properties of the intervertebral disc are determined by the interaction of the annulus fibrosus (AF), nucleus pulposus (NP), and end plate (EP) under different loading conditions. The interaction between these substructures enables the intervertebral disc to transfer the load. According to the principles of biomechanical adaptability and associated findings, skeletal cells such as fibroblasts, osteoblasts, and chondrocytes are sensitive to peripheral stress [8−12]. They not only experience stress changes, such as alterations in density and elastic modulus of extracellular matrix, in peripheral biomechanical environments but also use these environments to regulate stress. For example, synthesis of extracellular matrix increases density and elastic modulus, whereas decomposition has the opposite effect. Thus, these changes reduce or increase stress in the surrounding cells by building a micro-nano environment that facilitates cell survival. IVDD is the adaptive response of the intervertebral disc to excess stress that cells resist by synthesizing more extracellular matrix [8,9,11−13]. Consistently, a reduction in external stress can cause intervertebral disc cells to regulate their peripheral environment toward normalization. We hypothesized that accurate presentation of the micro-nano structural characteristics of the degenerative disc, including early identification of IVDD changes, and evaluation of specific substructural areas, could improve the Pfirrmann grading system.

Materials and methods

Animal models and experimental groups

In this study, 35 fully grown, 12-week-old male Sprague-Dawley rats (mean ± standard deviation weight 400 ± 15 g) were used. All animal experiments were approved by the Institutional Animal Care Committee of the Laboratory Animal at the School of Medicine, SooChow University (Suzhou, China). Rats were assigned randomly to one of five groups (n = 7 per group): control (no intervention to the intervertebral disc of the tail), and four intervention groups that all had caudal vertebrae immobilized using a custom-made external device to fix four caudal vertebrae (Co7−Co10; Fig. 1), but with variable subsequent compression of Co8 and Co9 for 2 weeks, 4 weeks, 6 weeks, or 8 weeks. MRI

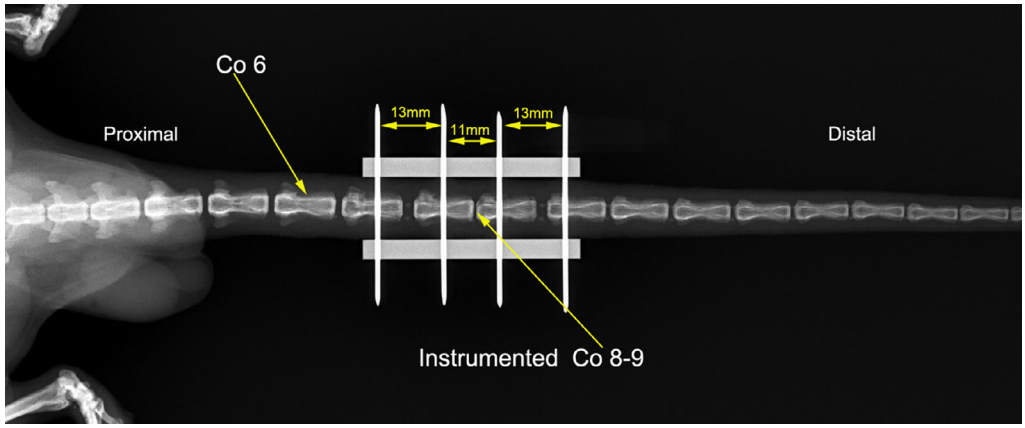

Fig. 1. X-ray image of the loading device fixation. In the model, four K-wires (50 mm in length and 1.2 mm in diameter) were fixed in parallel using two aluminum alloy cuboids (43 mm in length, 4 mm in width, net weight 5.0 g). The hole spacing of Co8 and Co9 was 11 mm, and the hole spacing of Co7 and Co8 and Co9 and Co10 were both 13 mm. After the mechanical test, the compression force of Co8 and Co9 was 22 N.

detection of rat coccygeal vertebrae was conducted at each time node of the experiment, and the T2 signal intensity and disc space were evaluated. At termination of the experiment, animals were euthanized and the caudal vertebrae were harvested for further analysis. Histopathology, glycosaminoglycan (GAG) content, histologic score, EP structure, and elastic modulus of the intervertebral disc were evaluated.

MRI scanning and GAG assay

The intervertebral disc specimens of rat caudal vertebrae were scanned in a 1.5T MRI scanner (GE HDE, scanning sequence: FRFSE-XL, scanning orientation: sagittal plane, slice thickness: 1.4 mm), and scored by three radiologists and three spinal surgeons using the Pfirrmann system (Fig. 2). NP samples (n = 20) underwent papain (Shanghai Yuanye Bio-Technology Co Ltd, Shanghai, China) digestion in 1.0 mL of 20 mM sodium phosphate buffer (1 mM ethylenediaminetetraacetic acid, 2 mM dithiothreitol, and 300 μg papain) at 65°C for 2 hours. GAG content was calculated with chondroitin-4 sulfate as the standard and based on the dimethylmethylene blue method [14]. To standardize GAG values, the DNA concentration of each sample was measured using PicoGreen analysis [15].

Histologic analysis

After completion of each time node, the animals were euthanized by an excess of isoflurane (RWD Life Science Co, Shenzhen, China). There were three samples in each group, and a total of 15 samples were used for histologic analysis. The target coccygeal vertebrae (Co8 and Co9) were harvested, fixed in 10% buffered formalin solution (Shanghai Yuanye Bio-Technology Co Ltd, Shanghai, China) for 24 hours, and decalcified in 10% ethylenediaminetetraacetic acid (Biosharp, Hefei, China) for 30 days. The discs were then paraffin-embedded (Leica, Richmond, USA), and 5-μm-thick sagittal plane sections prepared using histotome (Leica, Heidelberger, Germany) with 20 pieces cut from each specimen. For histologic analysis, sections were stained with hematoxylin/eosin (Beijing Biotopped Science & Technology Co Ltd, Beijing, China). Staining was evaluated using a binocular microscope (XSP-2CA, Shanghai, China). Histologic evaluation was based on a grading system developed by Han et al. [16]. The number of cells in the NP was

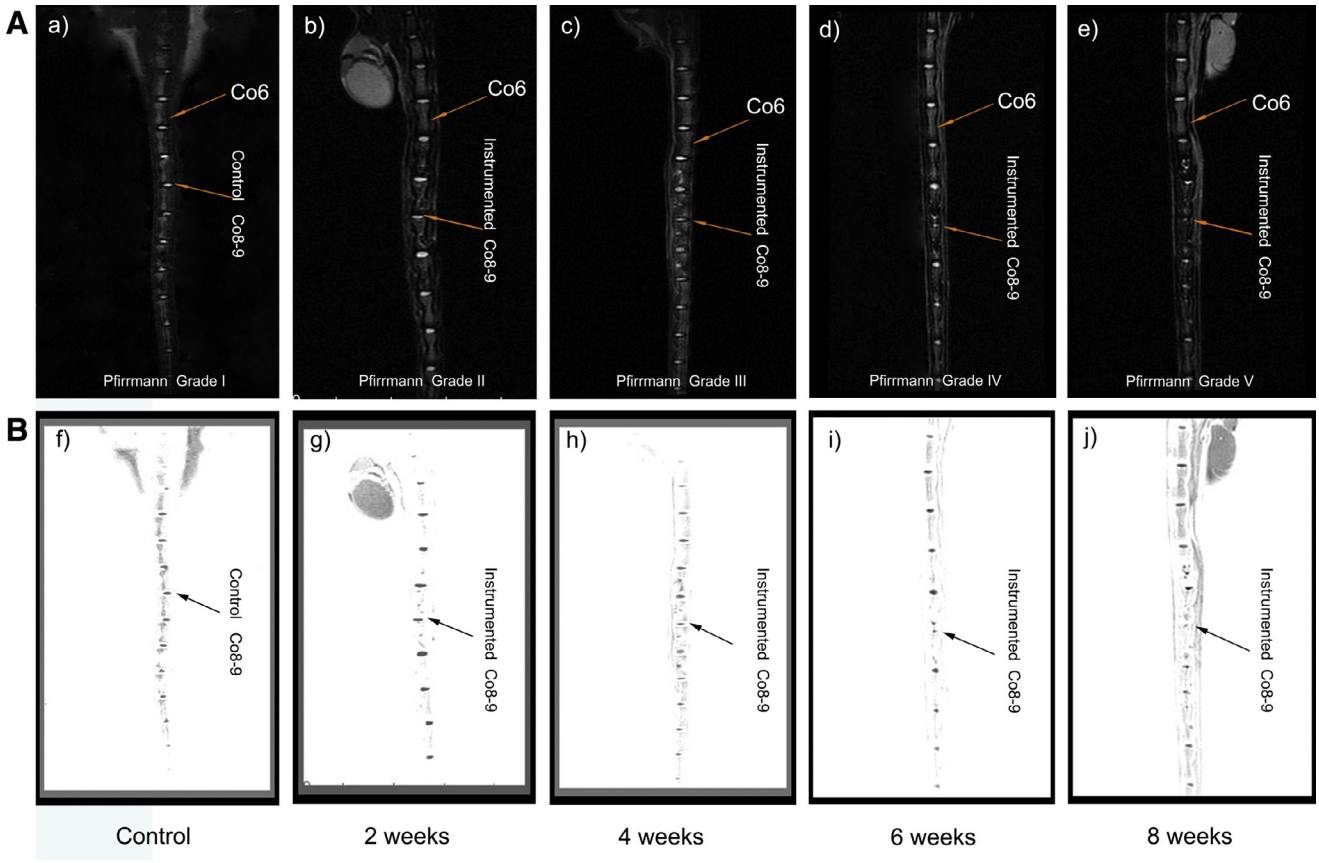

Fig. 2. Correlation between disc degeneration and Pfirrmann grade. MRI scans (scanning sequence: FRFSE-XL, scanning orientation: sagittal plane, slice thickness: 1.4 mm) used magnetic waves to create pictures to determine NP size and hydration status according to T2 signal intensity. Based on Pfirrmann grade, after 2, 4, 6, and 8 weeks of compression, Co8 and Co9 disc degeneration reached Pfirrmann grades II, III, IV, and V, respectively. The figures in row B (Fig. f–j) are the corresponding inverse color image from row A (Fig. a–e).

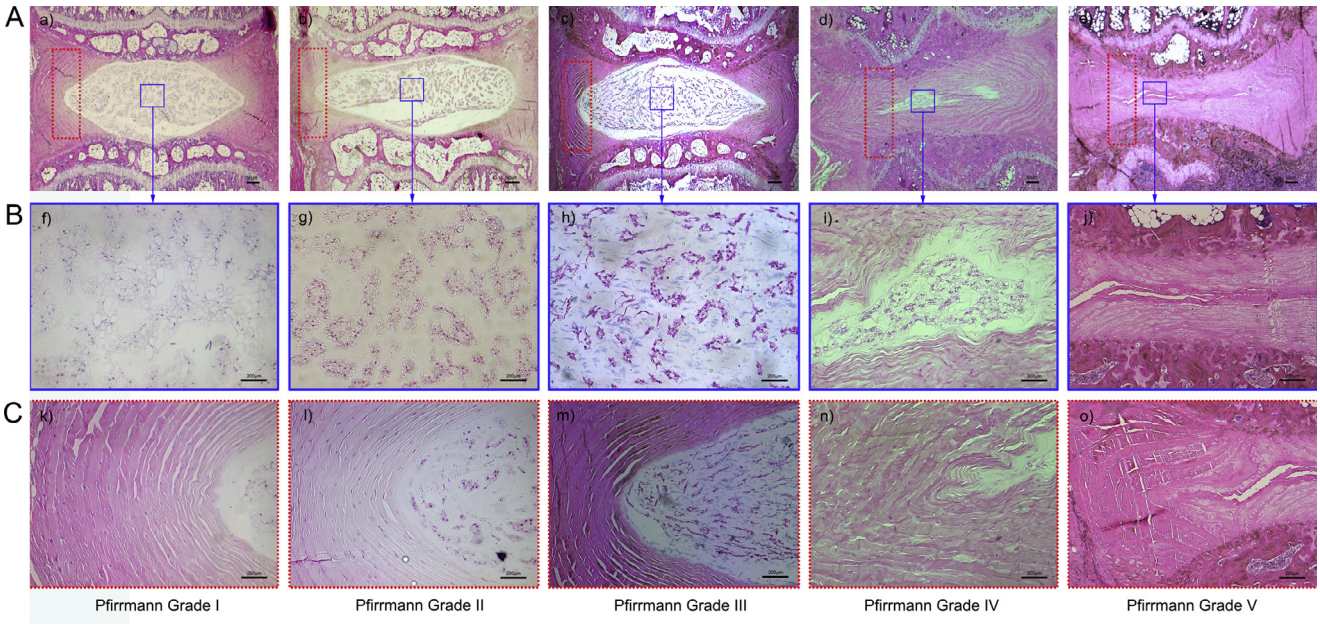

Fig. 3. Histologic analysis of intervertebral discs based on Pfirrmann grade. Hematoxylin/eosin (HE) stain. (A) Figure a–e, intervertebral disc under magnification (50×). (B) Figure f–j, intervertebral disc at higher magnification (200×). (C) Figure k–o, intervertebral disc at magnification (200×). The figures in row B are enlarged images of the blue solid line box in row A. The figures in row C are enlarged images of the red dotted rectangle in row A.

recorded by counting from the hematoxylin-/eosin-stained images at a magnification of 200× (Fig. 3f–j).

Evaluation of bony EPs by scanning electron microscopy

After the rats were euthanized, the coccygeal vertebrae (Co8 and Co9) were removed, along with the surrounding tissues including ligaments, intervertebral discs, spinal cord, and nerve roots. The Co8 and Co9 vertebrae (n = 4 per group, a total of 20 samples) were placed into pre-prepared test tubes containing 20 mL of a mixed enzyme solution comprised of type I and type II collagenase (NY Life Technologies Co, Grand island, NY, USA). Type I and II collagen were added, at 0.05 g each, to make 0.5% mixed solution in 20 mL phosphate buffered solution. The tubes were then placed in a 37°C incubator, with the enzyme solution replaced every 2 days until day 6 when the soft tissue and cartilage on the surface of vertebral specimens were digested and the bony EP integrity was preserved. After repeated washing with sodium chloride 0.9%, bony EP specimens were dehydrated using a gradient of 70%, 80%, and 90% ethanol, after which the specimens were placed in a cool, ventilated area and dried for 24 hours. At this point, the bony EPs were generally separated from the vertebral body. According to our previous experimental work and relevant references, Sputtering Coater (SC7620, Quorum Technologies Ltd, East Sussex, UK) was used to evenly spray gold for 45–60 seconds on the Co8 and Co9 intervertebral space cranial EP (n = 4 per group, a total of 20 samples) before observation by scanning electron microscopy (FEI Quanta 250, Hillsboro, USA, Fig. 5A).

Atomic force microscopy (AFM) imaging and nanomechanical testing

The AFM scanner (Dimension ICON, Bruker, Billerica, MA, USA) was used at atmospheric pressure. The structure and elastic modulus of the individual collagen fibrils within the AF of intervertebral discs Co8 and Co9 were tested at nanoscale using AFM in weeks 0, 2, 4, 6, and 8 (Fig. 6). Because the properties of collagen fibrils may vary at different locations within the AF, explanted samples were divided into two scanning areas as shown in Fig. 7. The samples were analyzed blindly based on our previous research experience (n = 4 per group, a total of 20 samples) [17–19]. Sites A and B were designated as the outer and inner layers of the AF, respectively. Both AFM imaging and nanomechanical testing were conducted at a scanning rate of 1 Hz using a Scan Asyst-Air probe, a curvature radius of 5 nm and a force constant of 0.4 N/m.

Statistical analysis

Data management and statistical analysis were performed using Excel 2016 (Microsoft Corp., Redmond, WA, USA) and SPSS 24.0 (IBM SPSS Inc, Chicago, IL, USA). Data are presented as mean ± standard deviation. Significant differences between study groups were evaluated using one-way analysis of variance. If there were statistical differences, we performed homogeneity of variance testing and obtained the homogeneity of variance. Tukey's multiple comparisons test was used to analyze the influence of compression loads and time. Statistical significance was set at $p \leq .05$.

Results

A total of 35 rats across five groups participated in and completed the experiment. MRI images of the intervertebral discs were evaluated in a double-blind fashion by three radiologists and three spine surgeons all of whom had years of working experience. These experts evaluated the degree of degeneration and Pfirrmann grade in the 35 rats, with consistent assessments in 32 rats and controversial assessments in three rats. We then adopted the principle of majority rules to evaluate. The experts agreed that the control group was classified as Pfirrmann grade I. After 2, 4, 6, and 8 weeks of compression, Co8 and Co9 disc degeneration reached Pfirrmann grades II, III, IV, and V, respectively (Fig. 2).

NP presented cell clusters at Pfirrmann grade II, with large, vacuolated notochord cells replaced by small, less active mature NP cells. IVDD was observed at an earlier Pfirrmann grade under the microscope. Disc degeneration is a dynamic process. After 2 weeks of compression, the intervertebral disc passed from Pfirrmann grade I to grade II (Pfirrmann grade I and II is defined clinically as "normal"). At this point, the decrease in proteoglycans and the loss of water content caused abnormal regeneration of NP to occur in cell clusters. Large, vacuolated notochord cells were replaced by small, less active mature NP cells, and the density of NP cells increased gradually showing an uneven distribution (Fig. 3b, g, and l). The number of functional cells decreased from 1,404 at Pfirrmann grade I to 1,244 at grade II ($p \leq .05$; Fig. 4A). Histologic score ranged from 5.21 at Pfirrmann grade I to 5.57 at grade II ($p \leq .05$; Fig. 4B). However, the total GAG content of the NP was not significantly different between Pfirrmann grades I and II ($p > .05$; Fig. 8). After 4 weeks of compression, IVDD worsened to Pfirrmann III (early clinical degeneration, Fig. 3c, h, and m). At this stage, the NP showed a typical cell cluster phenomenon caused by the obvious loss of water content. NP cell density was lower than occurred in grades I and II. The NP and the AF inner layer began to appear disordered with fissure formation (Fig. 3c, h, and m). The total GAG content of the NP in rats in Pfirrmann grade III decreased significantly compared with rats in the Pfirrmann grade II ($p < .0001$; Fig. 8). After 6 weeks of compression, IVDD deteriorated to Pfirrmann grade IV (middle and late stages of clinical degeneration). NP cell density was significantly lower than in grades I–III. NP volume and the total GAG content were also decreased further, the inner and outer AF layers were disordered obviously, and the boundary between NP and AF was blurred. Part of the NP was replaced by disordered granulation and scar tissue (Fig. 3d, i, and n). The cartilage EP had obvious fibrosis and the intervertebral space had light to moderate stenosis. After 8 weeks of compression, IVDD worsened to Pfirrmann V (late stage degeneration), NP water content had almost completely disappeared, and NP was almost entirely replaced by the structural disorder of granulation and scar tissue. Compared with Pfirrmann grades I–III, the total GAG content of the NP of Pfirrmann grade V rats was reduced significantly ($p < .0001$; Fig. 8). However, the total GAG content of the NP was not significantly different between Pfirrmann grades IV and V ($p > .05$). Additionally, there was little or no trace of cells but there was extensive AF fibrosis, obvious EP sclerosis and collapse, and the histologic score rose to 14.43 (Figs. 3e, j, and o, and 4B).

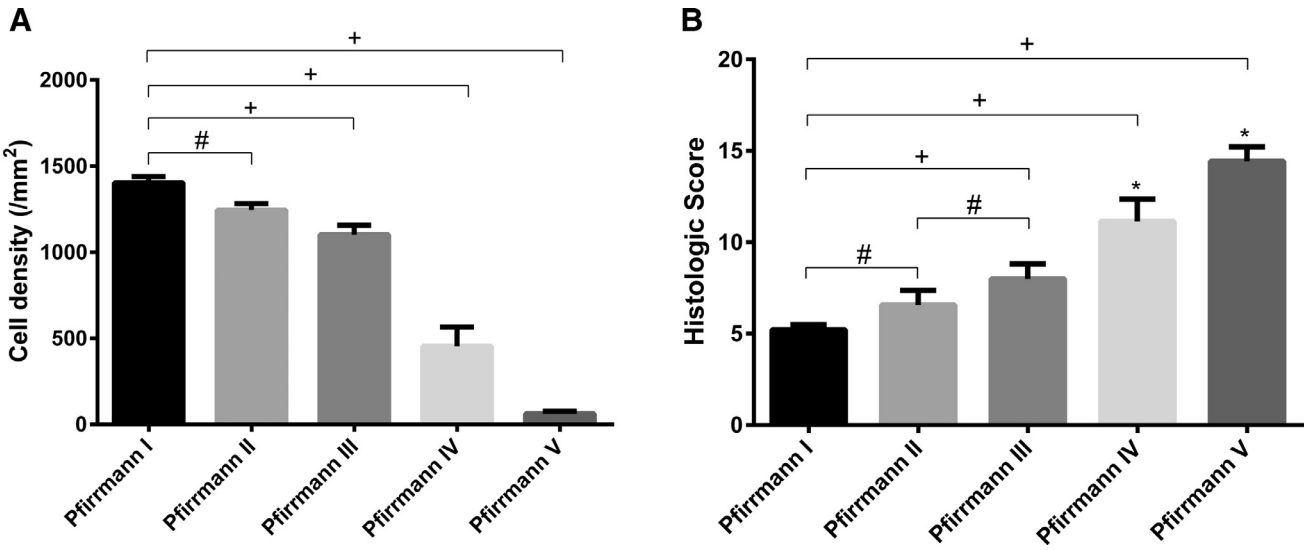

Fig. 4. Density analysis of NP cells based on Pfirrmann classification. (A) Comparison of the number of NP cells after compression of intervertebral discs. (#) indicates significant difference between groups ($p \leq .05$). (+) indicates significant difference between groups ($p \leq .0001$). (B) Histologic evaluation was based on the grading system developed by Han et al. (#) indicates significant difference between groups ($p \leq .05$). (+) indicates significant difference between groups ($p \leq .0001$). (*) indicates significant difference from other groups ($p \leq .0001$).

Pore structure of the bony EP did not change significantly at Pfirrmann grades I and II, but the number of pores decreased gradually with an increase in Pfirrmann grade (grades III−V). There was irregular progress in wormlike destruction of the rough EP surface, calcification, and hardening of the EP with osteophyte formation, and the central EP area was more obvious than the peripheral area. The bony EP structure of the EP-intervertebral disc interface of unloaded discs contained a large number of regular pores with a "concave lens" shape (Fig. 5A; a−c). After 2 weeks of compression loading, the vertebral EP structure did not present with the typical qualitative changes compared with control group (Fig. 5A; d−f). After 4 weeks of compression loading, the pore structure was progressively ablated and increasingly irregular with rough EP surfaces also following this pattern. The central EP area was more obvious than its surroundings, and there was a significant reduction in the number of pores with a "concave lens" shape along with increased calcification and osteophyte formation (Fig. 5A; g−i). A comparison of the number of pores in the EP-intravertebral disc interface of the bony EP is shown in Fig. 5B. By increasing the compression time to 6 and 8 weeks (Pfirrmann grades IV and V), the rat bony EP structure showed further deterioration that positively correlated with time (Fig. 5A; j−o).

The AF elastic modulus and the collagen fiber diameter differed significantly with increasing Pfirrmann grade. Representative AFM images of collagen fibrils from intervertebral discs of Pfirrmann grades I−V are shown in Fig. 6, with outer and inner layers of the left side surface of the AF shown at high resolution (1×1 μm) as site A and B in Fig. 7. After compression loading of 22 N for 2−8 weeks, the individual AF fibrils were significantly thicker than those in the control group. The collagen fibril diameters of the AF at different scanning sites are shown in Fig. 9A and B. For both Pfirrmann grades I−V, the fibril diameters increased significantly in the outer layer compared with the inner layer. After compression for 2 weeks (Pfirrmann grade II), fibril diameters exhibited no significant change compared with the control group (Pfirrmann grade I). For the 4, 6, and 8 weeks groups (Pfirrmann grades III−V), average fibril diameter increased significantly ($p < .05$). The results showed that there were significant differences in the diameter of collagen fibers with different positions and compression periods. The elastic modulus of collagen fibrils from different regions within the AF is shown in Fig. 10A and B. For both the control and loaded groups, the fibrils in the outer layers were stiffer than those in the inner layer ($p < .05$). In the 2 weeks group (Pfirrmann grade II), the average elastic modulus of fibrils exhibited a significant increase in the outer layers compared with the control group (Pfirrmann grade I, $p < .05$), but the inner layer did not differ. In the 4 weeks group (Pfirrmann grade III), the average elastic modulus of fibrils was significantly increased in the outer layers compared with the control group (Pfirrmann grade I, $p < .05$), but the inner AF layer was not different. In the 6 and 8 weeks groups (Pfirrmann grades IV and V), the collagen fibrils were both significantly stiffer in the outer and inner layers ($p < .05$). There was also a significant increase in fibril modulus with increasing Pfirrmann grades of I, II, and V ($p < .05$). The results showed that under the condition of constant compression loads, the scanning position and compression period influenced individual fibril stiffness significantly.

Discussion

Our study found that the Pfirrmann grading system combined with intervertebral disc micro-nano structural changes more comprehensively reflected the extent of disc degeneration.

IVDD is a cell-mediated cascade of biochemical, mechanical and structural changes occurring under abnormal intervertebral disc stress [20]. It is an accelerated normal aging process involving self-correction of the intervertebral disc under a stress load that leads to compromised disc function [21]. According to the Pfirrmann grading system, grades I and II are normal intervertebral discs, with the difference between these grades related mainly to whether the high NP signal is completely homogeneous rather than where there are differences in strength (intensity). Our study confirmed that, at Pfirrmann grade II, there were cell clusters in the NP, the proportion of notochord cells with large vacuolar morphology in the NP was decreased, and the proportion of mature NP cells with small morphology and low metabolic activity was increased. This was consistent with Guehring's research [22]. At this grade, the average elastic modulus of fibrils exhibited a significant increase in the outer layers compared with the control group (Pfirrmann grade I). There was no obvious degeneration in bony EP. At Pfirrmann grade III, NP had a further reduction in moisture content, total GAG content and cell apoptosis. These changes were consistent with findings presented in previous studies showing that proteoglycan loss occurs during the initial stage of disc degeneration [15,23]. It also confirmed that the bony EP began to undergo micro-nano scale reconstruction. This was seen as the number of micropore channels decreased gradually and the nutrient metabolism of NP became further disordered. Meanwhile, there was a significant increase in the fibril modulus of the AF outer layers, without a change in the mechanical properties of the inner layer. The results indicated that, at the early stages of clinical degeneration of the intervertebral discs (Pfirrmann grades II and III), there were already significant changes in mechanical properties of the outer AF layer compared with the inner layer. Pfirrmann grade IV is the middle and late stage of degeneration. NP cell density and activity decreased significantly, and NP nutrition and metabolic disorder intensified. Both outer and inner layers of the AF had altered mechanical properties, whereas the EP micropore channel became further blocked and finally closed completely as the intervertebral

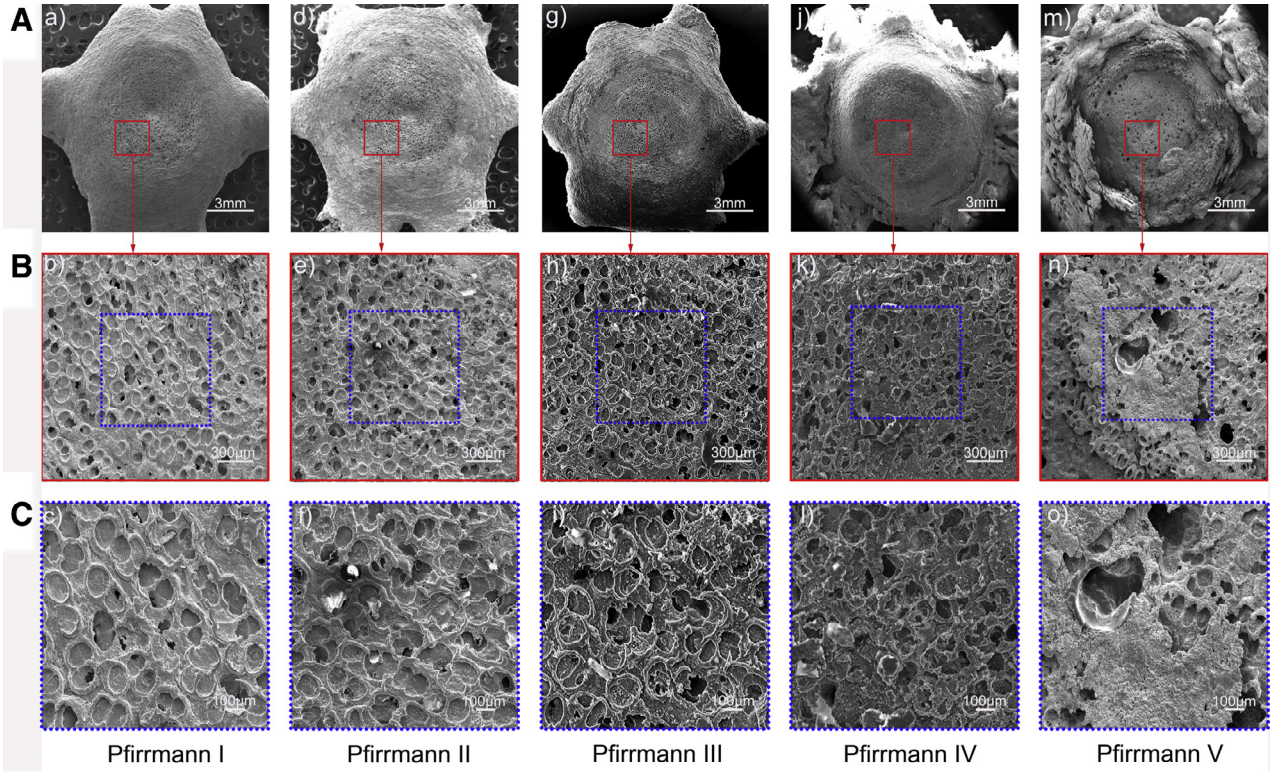

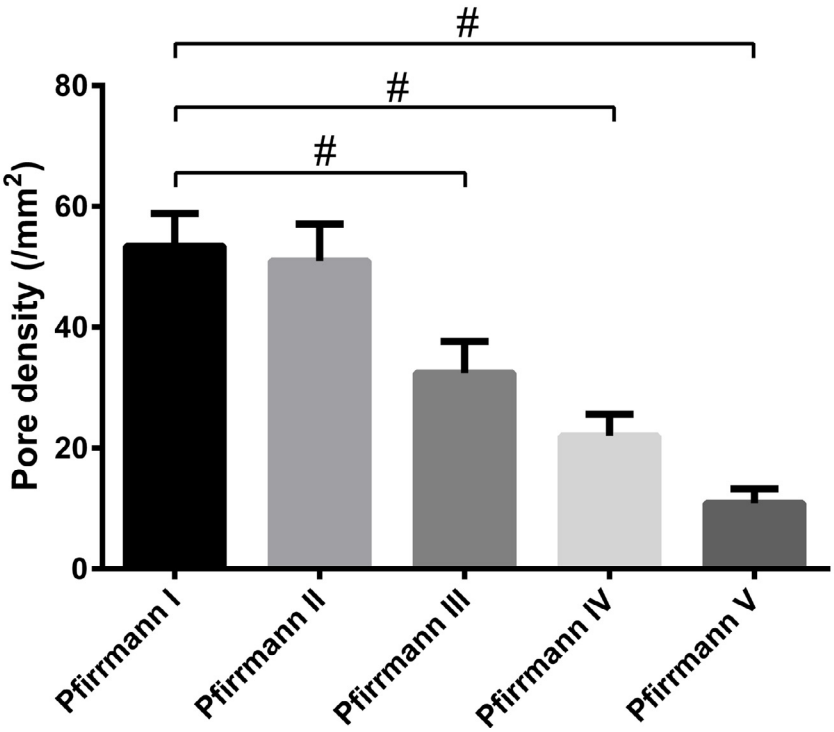

Fig. 5. Morphologic and structural changes of the EP during disc degeneration. (A) a–c: control (Pfirrmann grade I); d–f: 2 weeks (Pfirrmann grade II); g–i: 4 weeks (Pfirrmann grade III); j–l: 6 weeks (Pfirrmann grade IV); m–o: 8 weeks (Pfirrmann grade V). The overall structure of the EP indicates that the micropores are all concentrated in the central position where the EP is connected to the NP. The figures in row B are enlarged images of the red solid line rectangle in row A. The figures in row C are enlarged images of the blue dotted rectangle in row B. B. Changes in the number of pores in the bony EP. (#) indicates significant difference between groups ($p \leq .0001$).

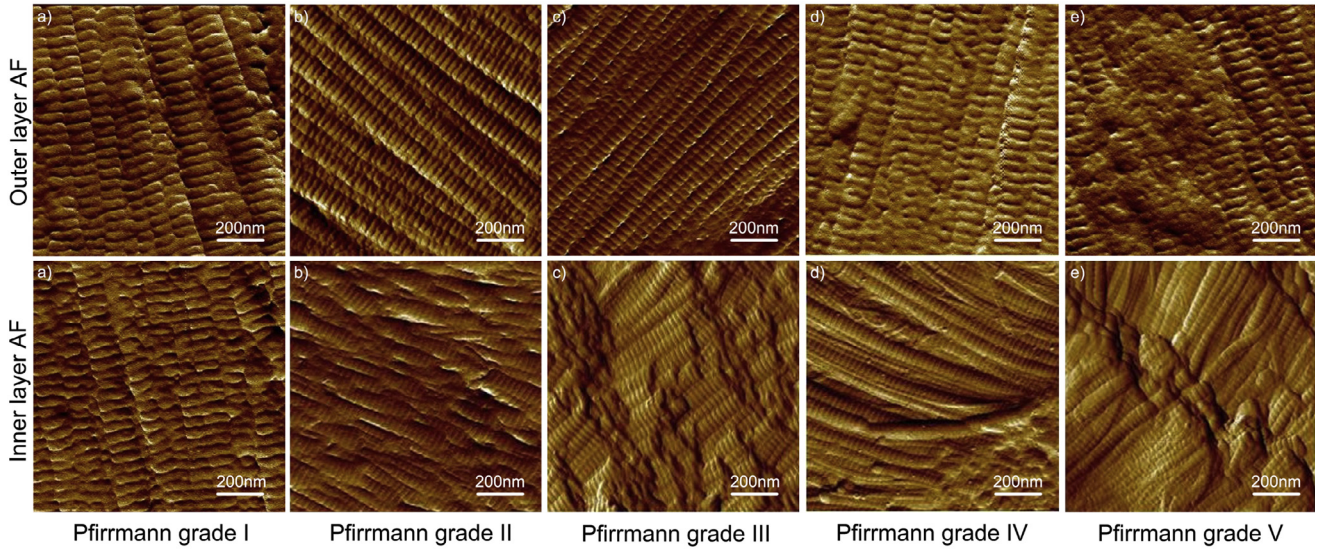

Fig. 6. Atomic force microscopy (AFM) was used to observe the microstructure of AF collagen fibers over time. Representative AFM images of collagen fibrils in the AF of the intact disc and the degenerated discs after bearing compression for 2, 4, 6, and 8 weeks. All images were scanned in the outer layer (site A) and inner layer (site B) on the AF.

disc became necrotic. Pfirrmann grade V is based on grade IV, but with EP collapse. In this stage, the boundary between NP and AF was not clear, and the intervertebral disc and EP were hardened. This meant that the specimens were difficult to obtain.

IVDD is a continuous process where microenvironmental cellular changes in the intervertebral disc substructure occur gradually over decades to eventually cause structural rupture and functional damage. It is difficult for MRI images to accurately reflect these changes [4]. Thus the Pfirrmann grading system, which is based on MRI images, cannot precisely identify the biomechanical micro-nano environmental changes of the intervertebral discs [5].We found that the bony EP structure did not undergo obvious degeneration in early clinical degradation (Pfirrmann grades I and II). More specifically, intervertebral disc tissue morphology and changes in cell number were not consistent in these early stages. However, during the clinical degeneration stages (Pfirrmann grades III−V) changes in structural form occurred alongside disc degeneration with ongoing compression stress of the intervertebral disc. This is consistent with the principle of biomechanic adaptability. Therefore, we believe that IVDD is not a simple structural abnormality, but a self-adaptive process developed with the change in biomechanical micro-nano environment. The intervertebral disc is anisotropic homogeneous biological tissue with biomechanical properties that change with variation in load, location, and duration in the micro-nano scale. Therefore, this information cannot be obtained from macroscopic clinical testing [8]. More importantly, induction and regulation of the outside world by cells, under the biomechanical adaptation principle, occurs within this scale and cannot be detected macroscopically [11,24−26]. The observations regarding AF morphology, structure, and elastic modulus in this study showed that the diameters and fibril modulus of the outer and inner layers of AF collagen fibers changed significantly with increasing Pfirrmann classification. These results showed that there was a significant difference in the elastic modulus and diameter of collagen fibers with different location and duration. These findings not only confirm the existence of macroscopic differences in the biomechanical micro-nano environment, but also the ability of cells to sense and self-regulate this environment including elastic modulus and structural parameters such as collagen fiber diameter. Because elastic modulus is known to sense peripheral stress in cells, the biomechanical induction of cells changes with variation in location. Therefore, we believe that there is a significant difference in the biomechanical micro-nano environment distribution of the degenerated intervertebral disc including the elastic modulus and structure [17,18]. As a result, IVDD eventually leads to a change in the overall intervertebral disc structure through changes in various substructure-related characteristics.

Each part of the substructure of the intervertebral disc has its unique mechanical properties. Degeneration affects the mechanical properties of the intervertebral disc tissue, which is then reflected by the mechanical properties of the entire intervertebral disc. Thus, damage to the mechanical properties of one component will result in damage to the overall mechanical function of the intervertebral disc. A recent study suggested that degeneration of the AF may be the origin of lower back pain in patients with degenerative disc disease [27]. Under MRI-T2, the AF (especially the outer AF) is shown as a dark area, which does not

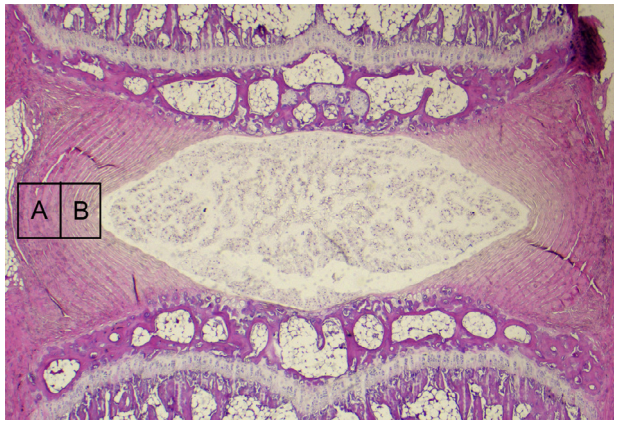

Fig. 7. Schematic of the different scanning regions in the AF using atomic force microscopy. Outer layer (site A) and inner layer (site B) on the AF.

accurately indicate the morphologic structure of the AF. This is one of the reasons why the Pfirrmann grade, which is based on MRI images, cannot diagnose IVDD and its clinical symptoms accurately. This study confirmed that, at an early stage of clinical IVDD (Pfirrmann grades II and III), there will already have been significant changes in mechanical properties of the outer AF compared with the inner layer. This is consistent with the findings of Yonghing and Kirkaldy-Willis who reported that IVDD initially occurs in the outer AF [28]. In addition, Kuslich et al. reported that the posterior AF is the area responsible for lower back pain through identifying that stimulating the AF behind the herniation of the intervertebral disc can cause significant lower back pain [29]. It is also known that the relationship between EP and IVDD is close [30], with the EP important for maintaining integrity of the intervertebral

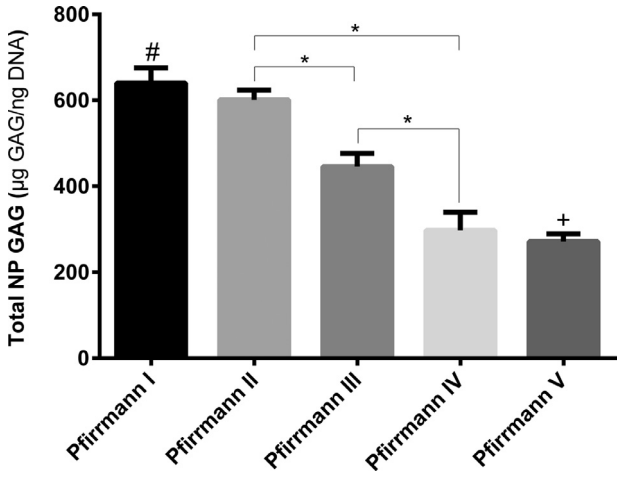

Fig. 8. Glycosaminoglycan (GAG) assay. (#) indicates significant difference from other groups, except for Pfirrmann grade II ($p \leq .0001$). (*) indicates significant differences between groups ($p \leq .0001$). (+) indicates significant difference from other groups, except for Pfirrmann grade IV ($p \leq .0001$).

disc structure and its physiological function [31,32]. Under MRI-T2, EPs are displayed as dark areas. EP damage can change the mechanical properties of the intervertebral disc that is difficult to detect on MRI and consequently poorly accommodated by the Pfirrmann grading system. Visualization of the morphologic EP defects can help clarify the etiology of IVDD and related diseases [21,33]. Wang et al. found lesions in nearly half of the lumbar vertebral body EPs in a study of a lumbar spine specimen (n = 150) database. This suggested that the incidence of EP lesions in the clinical MRI study was seriously underestimated [34]. We understand that the intervertebral discs are the body's largest structure without blood supply [35,36], with nutritional supply mainly from EP diffusion [3,31]. Therefore, degeneration of the EP structure leads to closure of nutrient channels [37,38]. Insufficient nutrient supply results in NP degeneration [34,39,40]. Gruber et al. demonstrated that nutrients in the intervertebral disc do not pass through blood vessels but penetrate through the hard bone surface to the EP directly [41]. Once the EP calcifies and is replaced by hard bone, nutrient diffusion to the intervertebral disc ceases [42,43]. Takatalo et al. confirmed that the appearance of Schmorl nodules was closely related to intervertebral disc deformation and discogenic back pain [44,45]. Therefore, clarification of the EP structural changes will help to further explain the etiology of IVDD [2,34,46,47]. This study confirmed that in early clinical IVDD (Pfirrmann grade III), the pore structure of the bony EP is changed significantly compared with controls (Pfirrmann grade I). This further confirmed that the bony EP, at this grade, began to undergo micro-nano scale reconstruction. This suggests that if we can intervene before EP calcification, IVDD may not develop seriously. In other words, early intervention for EP calcification may delay disc degeneration or even regenerate discs.

Limitations of the study

This is a basic science study focused on Pfirrmann grade, and cannot yet be used in the clinic. However, we intend to provide further biomechanical information for Pfirrmann grading and the clinical diagnosis of degenerative disc disease through this line of research. Therefore, we used the rat caudal vertebral model to evaluate micro-nano environment changes in the intervertebral disc. Although not completely equal to human intervertebral disc changes, the rat model is the currently accepted model and was easier to build and replicate than alternatives. More importantly, it provided relevant experimental parameters of intervertebral disc substructure corresponding to Pfirrmann grade that human intervertebral discs cannot provide. As a result, we are confident that the changes observed in the intervertebral disc micro-nano environment in rats combined with the classical Pfirrmann grade will help to further elucidate the etiology of human IVDD and related secondary diseases.

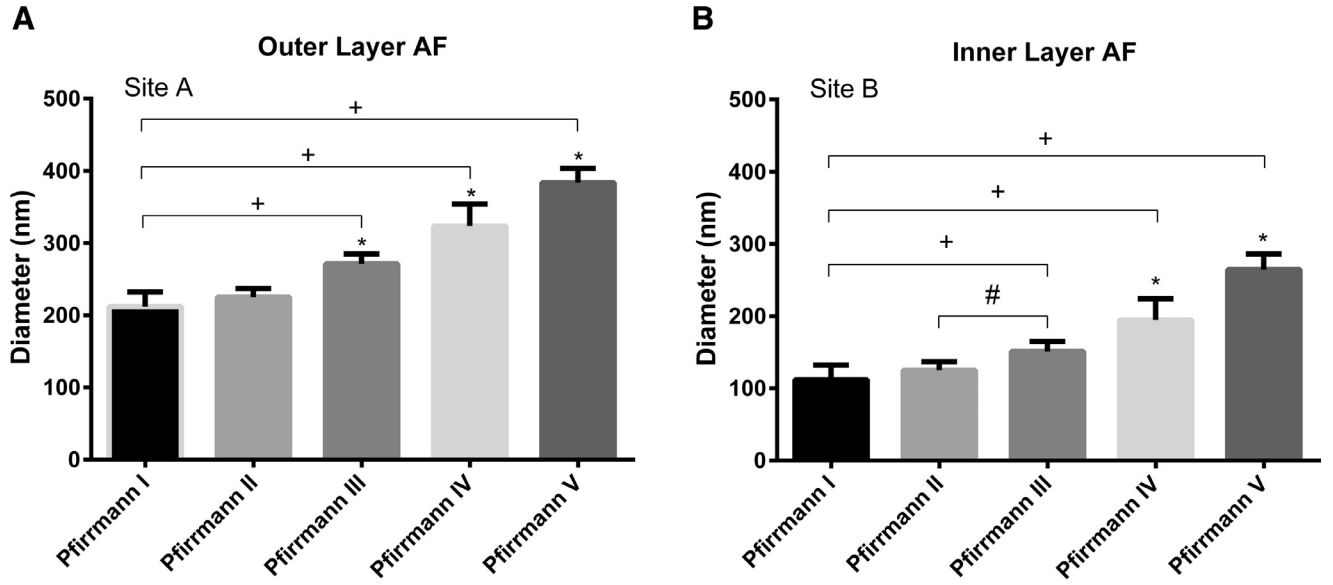

Fig. 9. Mean diameters of collagen fibrils with different compressive duration in AF (n = 20). The fibril diameters were analyzed from outer layer (site A) to inner layer (site B). (#) indicates significant difference between groups ($p \leq .05$), (+) indicates significant difference between groups ($p \leq .0001$), (*) indicates significant difference from other groups ($p \leq .0001$).

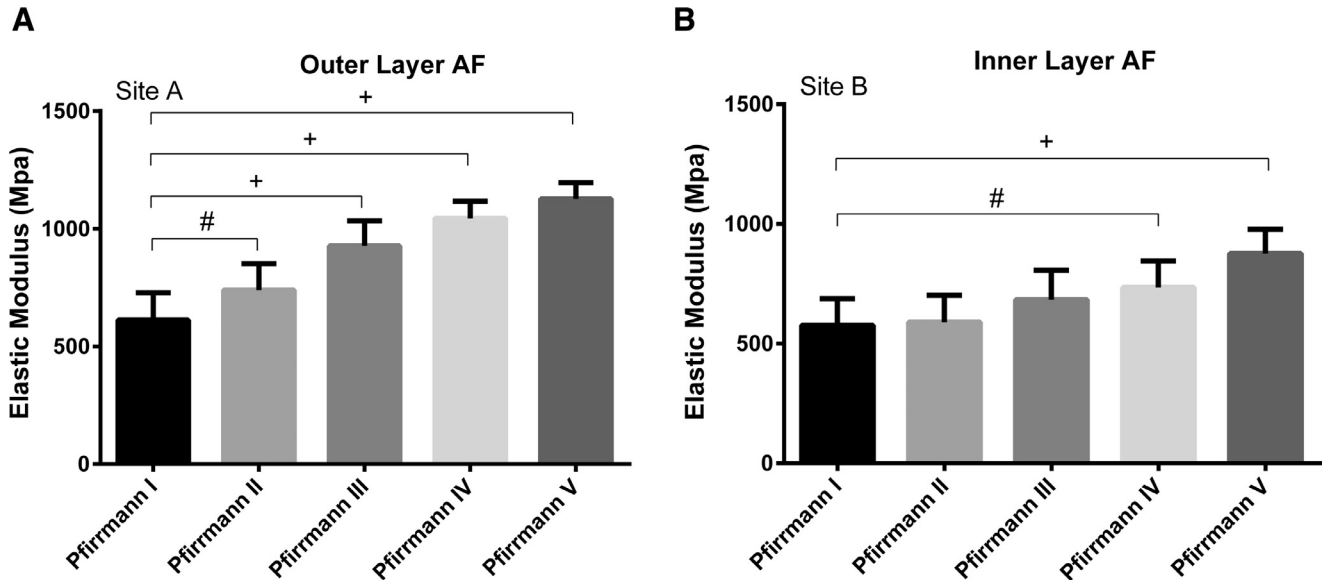

Fig. 10. Mean elastic modulus of collagen fibrils with different Pfirrmann grades (n = 20). The elastic modulus was analyzed from outer layer (site A) to inner layer (site B). (#) indicates significant difference between groups ($p \leq .05$), (+) indicates significant difference between groups ($p \leq .0001$).

Conclusions

In this study, changes to the intervertebral disc micro-nano environment based on Pfirrmann grade were used to determine that early IVDD occurs when the NP is defined as normal clinically (Pfirrmann I and II). It was revealed that changes in the Pfirrmann classification and intervertebral disc micro-nano structure were not synchronous in the early stages of IVDD. Evaluation of the micro-nano changes in substructures such as EPs and AF at different Pfirrmann grades improved ability to understand pathogenesis and process of IVDD. These results indicated that disc degeneration is not just a macroscopic MRI view of NP dehydration, but that it also involves micro-nano scale changes to the morphology and biomechanics of substructures such as AF and EPs. This work provides further information on AF and EPs at the micro-nano

level and contributes to determination of the etiology of IVDD.

Acknowledgments

This study was funded by the National Natural Science Foundation of China (81320108018, 31570943, and 81702146), Innovation and Entrepreneurship Program of Jiangsu Province, and Basic Research Program of Jiangsu Province (BK20180196).

Competing interests

None.

Supplementary materials

Supplementary material associated with this article can be found, in the online version, at https://doi.org/10.1016/j.spinee.2019.01.008.

References

[1] Kettler A, Wilke HJ. Review of existing grading systems for cervical or lumbar disc and facet joint degeneration. Eur Spine J 2006;15:705–18.
[2] Rade M, Maatta JH, Freidin MB, Airaksinen O, Karppinen J, Williams FMK. Vertebral endplate defect as initiating factor in intervertebral disc degeneration: strong association between endplate defect and disc degeneration in the general population. Spine 2018;43:412–9.
[3] Huang YC, Urban JP, Luk KD. Intervertebral disc regeneration: do nutrients lead the way? Nat Rev Rheumatol 2014;10:561–6.
[4] Schneiderman G, Flannigan B, Kingston S, Thomas J, Dillin WH, Watkins RG. Magnetic resonance imaging in the diagnosis of disc degeneration: correlation with discography. Spine 1987;12:276–81.
[5] Pfirrmann CW, Metzdorf A, Zanetti M, Hodler J, Boos N. Magnetic resonance classification of lumbar intervertebral disc degeneration. Spine 2001;26:1873–8.
[6] Bertagnoli R, Kumar S. Indications for full prosthetic disc arthroplasty: a correlation of clinical outcome against a variety of indications. Eur Spine J 2002;11(Suppl 2):S131–6.
[7] Luoma K, Riihimaki H, Luukkonen R, Raininko R, Viikari-Juntura E, Lamminen A. Low back pain in relation to lumbar disc degeneration. Spine 2000;25:487–92.
[8] Vergroesen PP, Kingma I, Emanuel KS, Hoogendoorn RJ, Welting TJ, van Royen BJ, et al. Mechanics and biology in intervertebral disc degeneration: a vicious circle. Osteoarthritis Cartilage 2015;23:1057–70.
[9] Chaudhuri O, Gu L, Klumpers D, Darnell M, Bencherif SA, Weaver JC, et al. Hydrogels with tunable stress relaxation regulate stem cell fate and activity. Nat Mater 2016;15:326–34.
[10] Murphy WL, McDevitt TC, Engler AJ. Materials as stem cell regulators. Nat Mater 2014;13:547–57.
[11] Huebsch N, Lippens E, Lee K, Mehta M, Koshy ST, Darnell MC, et al. Matrix elasticity of void-forming hydrogels controls transplanted-stem-cell-mediated bone formation. Nat Mater 2015;14:1269–77.
[12] Oria R, Wiegand T, Escribano J, Elosegui-Artola A, Uriarte JJ, Moreno-Pulido C, et al. Force loading explains spatial sensing of ligands by cells. Nature 2017;552:219–24.
[13] Wuertz K, Godburn K, MacLean JJ, Barbir A, Donnelly JS, Roughley PJ, et al. In vivo remodeling of intervertebral discs in response to short- and long-term dynamic compression. J Orthop Res 2009;27:1235–42.
[14] Farndale RW, Buttle DJ, Barrett AJ. Improved quantitation and discrimination of sulphated glycosaminoglycans by use of dimethylmethylene blue. Biochim Biophys Acta 1986;883:173–7.
[15] Wei F, Zhong R, Zhou Z, Wang L, Pan X, Cui S, et al. In vivo experimental intervertebral disc degeneration induced by bleomycin in the rhesus monkey. BMC Musculoskelet Disord 2014;15:340.
[16] Han B, Zhu K, Li FC, Xiao YX, Feng J, Shi ZL, et al. A simple disc degeneration model induced by percutaneous needle puncture in the rat tail. Spine 2008;33:1925–34.
[17] Liang T, Zhang LL, Xia W, Yang HL, Luo ZP. Individual collagen fibril thickening and stiffening of annulus fibrosus in degenerative intervertebral disc. Spine 2017;42:E1104–11.
[18] Che YJ, Li HT, Liang T, Chen X, Guo JB, Jiang HY, et al. Intervertebral disc degeneration induced by long-segment in-situ immobilization: a macro, micro, and nanoscale analysis. BMC Musculoskelet Disord 2018;19:308.
[19] Liang T, Che YJ, Chen X, Li HT, Yang HL, Luo ZP. Nano and micro biomechanical alterations of annulus fibrosus after in-situ immobilization revealed by atomic force microscopy. J Orthop Res 2018. (Epub ahead of print) (PMID: 30370678 DOI: 10.1002/jor.24168) .
[20] Che YJ, Guo JB, Liang T, Chen X, Zhang W, Yang HL, et al. Controlled immobilization-traction based on intervertebral stability is conducive to the regeneration or repair of the degenerative disc: an in vivo study on the rat coccygeal model. Spine J 2018. (Epub ahead of print) (PMID: 30399448 DOI: 10.1016/j.spinee.2018.10.018).
[21] Adams MA, Roughley PJ. What is intervertebral disc degeneration, and what causes it? Spine 2006;31:2151–61.
[22] Guehring T, Urban JP, Cui Z, Tirlapur UK. Noninvasive 3D vital imaging and characterization of notochordal cells of the intervertebral disc by femtosecond near-infrared two-photon laser scanning microscopy and spatial-volume rendering. Microsc Res Tech 2008;71:298–304.
[23] Anderson DG, Tannoury C. Molecular pathogenic factors in symptomatic disc degeneration. Spine J 2005;5(6 Suppl):260S–6S.
[24] Bao G, Suresh S. Cell and molecular mechanics of biological materials. Nat Mater 2003;2:715–25.
[25] Luo ZP, An KN. A theoretical model to predict distribution of the fabric tensor and apparent density in cancellous bone. J Math Biol 1998;36:557–68.
[26] Wen JH, Vincent LG, Fuhrmann A, Choi YS, Hribar KC, Taylor-Weiner H, et al. Interplay of matrix stiffness and protein tethering in stem cell differentiation. Nat Mater 2014;13:979–87.
[27] Peng B, Hao J, Hou S, Wu W, Jiang D, Fu X, et al. Possible pathogenesis of painful intervertebral disc degeneration. Spine 2006;31:560–6.
[28] Yong-Hing K, Kirkaldy-Willis WH. The pathophysiology of degenerative disease of the lumbar spine. Orthop Clin North Am 1983;14:491–504.
[29] Kuslich SD, Ulstrom CL, Michael CJ. The tissue origin of low back pain and sciatica: a report of pain response to tissue stimulation during operations on the lumbar spine using local anesthesia. Orthop Clin North Am 1991;22:181–7.
[30] Wang Y, Videman T, Battie MC. ISSLS prize winner: lumbar vertebral endplate lesions: associations with disc degeneration and back pain history. Spine (Phila Pa 1976) 2012;37:1490–6.
[31] Wang Y, Battie MC, Boyd SK, Videman T. The osseous endplates in lumbar vertebrae: thickness, bone mineral density and their associations with age and disk degeneration. Bone 2011;48:804–9.
[32] Moore RJ. The vertebral endplate: disc degeneration, disc regeneration. Eur Spine J 2006;15(Suppl 3):S333–7.
[33] Urban JP, Winlove CP. Pathophysiology of the intervertebral disc and the challenges for MRI. J Magn Reson Imaging 2007;25:419–32.
[34] Wang Y, Videman T, Battie MC. Lumbar vertebral endplate lesions: prevalence, classification, and association with age. Spine 2012;37:1432–9.

[35] Holm S, Selstam G, Nachemson A. Carbohydrate metabolism and concentration profiles of solutes in the canine lumbar intervertebral disc. Acta Physiol Scand 1982;115:147–56.
[36] Grunhagen T, Shirazi-Adl A, Fairbank JC, Urban JP. Intervertebral disk nutrition: a review of factors influencing concentrations of nutrients and metabolites. Orthop Clin North Am 2011;42:465–77. vii.
[37] Benneker LM, Heini PF, Alini M, Anderson SE, Ito K. 2004 Young Investigator Award Winner: vertebral endplate marrow contact channel occlusions and intervertebral disc degeneration. Spine 2005;30:167–73.
[38] Hristova GI, Jarzem P, Ouellet JA, Roughley PJ, Epure LM, Antoniou J, et al. Calcification in human intervertebral disc degeneration and scoliosis. J Orthop Res 2011;29:1888–95.
[39] Takatalo J, Karppinen J, Niinimäki J, Taimela S, Näyhä S, Järvelin MR, et al. Prevalence of degenerative imaging findings in lumbar magnetic resonance imaging among young adults. Spine 2009;34:1716–21.
[40] Samartzis D, Karppinen J, Mok F, Fong DY, Luk KD, Cheung KM. A population-based study of juvenile disc degeneration and its association with overweight and obesity, low back pain, and diminished functional status. J Bone Joint Surg Am 2011;93:662–70.
[41] Gruber HE, Ashraf N, Kilburn J, Williams C, Norton HJ, Gordon BE, et al. Vertebral endplate architecture and vascularization: application of micro-computerized tomography, a vascular tracer, and immunocytochemistry in analyses of disc degeneration in the aging sand rat. Spine 2005;30:2593–600.
[42] Bernick S, Cailliet R. Vertebral end-plate changes with aging of human vertebrae. Spine 1982;7:97–102.
[43] Bernick S, Walker JM, Paule WJ. Age changes to the anulus fibrosus in human intervertebral discs. Spine 1991;16:520–4.
[44] Takatalo J, Karppinen J, Niinimäki J, Taimela S, Näyhä S, Mutanen P, et al. Does lumbar disc degeneration on magnetic resonance imaging associate with low back symptom severity in young Finnish adults? Spine 2011;36:2180–9.
[45] Takatalo J, Karppinen J, Niinimäki J, Taimela S, Mutanen P, Sequeiros RB, et al. Association of modic changes, Schmorl's nodes, spondylolytic defects, high-intensity zone lesions, disc herniations, and radial tears with low back symptom severity among young Finnish adults. Spine 2012;37:1231–9.
[46] Malandrino A, Lacroix D, Hellmich C, Ito K, Ferguson SJ, Noailly J. The role of endplate poromechanical properties on the nutrient availability in the intervertebral disc. Osteoarthritis Cartilage 2014;22:1053–60.
[47] Perilli E, Parkinson IH, Truong LH, Chong KC, Fazzalari NL, Osti OL. Modic (endplate) changes in the lumbar spine: bone micro-architecture and remodelling. Eur Spine J 2015;24:1926–34.